Recursive Memory-based Hysteresis Modeling for Solid-state Smart Actuators

SAEID BASHASH,[1] NADER JALILI,[1,*] PHILLIP EVANS[2] AND MARCELO J. DAPINO[2]

[1]*Smart Structures and NEMS Laboratory, Department of Mechanical Engineering, Clemson University Clemson, SC 29634 USA*

[2]*Smart Materials and Structures, Department of Mechanical Engineering, The Ohio State University Columbus, OH 43210, USA*

ABSTRACT: This article presents a new modeling approach for the memory-dependent hysteresis phenomenon in a broad class of smart structures and systems. We propose a recursive formulation to relate the minor hysteresis trajectories to their surrounding loops. More specifically, each internal (minor) trajectory targets its previous turning point and converges to its neighboring loop with a tunable exponential rate. By applying the 'curve alignment' and the 'wiping out' properties at the turning points, we present a new strategy within the context of a memory-based hysteresis modeling framework. A Galfenol-driven micropositioning actuator and a piezoelectrically driven nanopositioning stage are used to experimentally validate the model. Galfenol exhibits large butterfly-type nonlinearity with a small hysteresis effect, while the piezoelectric actuator exhibits wide hysteresis loops. The model is able to precisely predict the major and minor hysteresis loops in both the Galfenol and piezoelectric actuators, and is expected to be effectively and conveniently applicable to general systems exhibiting memory-dependent hysteresis.

Key Words: hysteresis modeling, smart materials, nano-positioning.

INTRODUCTION

SOLID-STATE smart actuators such as piezoelectric, magnetostrictive, electrostrictive, and shape memory alloy actuators are extensively utilized in many industrial and research-oriented devices. Their unique feature of offering ultra-accurate motions ranging from nanometer to millimeter enables many advantageous processes such as imaging, metrology, manipulation, manufacturing, and surgery. Hence, there is an increasing demand for the precise implementation of such devices in various state-of-the-art applications.

While these actuators deform at extremely small scales, their precision is limited by intrinsic nonlinearities such as hysteresis and creep. Hysteresis is an input/output multi-loop phenomenon with the presence of non-local memories (Krasnosel'skii and Pokrovskii, 1989; Bashash and Jalili, 2006). Future values of the output depend not only on the instantaneous value of the input but also on the material's history, especially the extremum points. If hysteresis is not carefully taken into account, large positioning errors occur which degrade the accuracy of the process. Hence, there is a need for accurate modeling of hysteresis in order to design efficient controllers.

There is a wide range of modeling frameworks for hysteresis in the literature. The most widely used classical models include the Preisach formulation (Ping and Musa, 1997; Tan and Baras, 2004) and its subclass the Prandtl-Ishlinskii operators (Kuhnen and Janocha, 2001; Bashash and Jalili, 2007c), the Duhem model (Stepanenko and Su, 1998), and the Maxwell slip model (Goldfarb and Celanovic, 1997). Because most of these conventional methods have rigid mathematical structures they tend to be complex to implement and to lack accuracy in practice. Moreover, they require a large number of parameters to accurately describe the experimental data. Hence, the system identification of such models is a significant issue in applications.

Several modeling approaches have been recently developed to provide better insight into the underlying physics of the hysteresis phenomenon using an energy-based approach (Smith et al., 2003a,b, 2006; Smith, 2005), and to improve the accuracy and the computational efficiency of modeling through a new memory-based paradigm (Bashash and Jalili, 2006, 2007a, 2008). The latter framework employs a set of intelligent hysteresis properties obtained from experimental

*Author to whom correspondence should be addressed.
E-mail: jalili@clemson.edu
Figures 1–13 appear in color online: http://jim.sagepub.com

1045-389X/09/18 2161–11 $10.00/0 DOI: 10.1177/1045389X09348927

observations on piezoelectric actuators, and develops a set of mathematical logics to describe these observations. These properties include 'targeting the turning points,' 'curve alignment,' and 'wiping out' effects at the turning points. The improvement of the proposed model over the classical methods has been shown in (Bashash and Jalili, 2008) for piezoelectric actuators. However, for different hysteretic systems such as magnetostrictive actuators, where the nonlinearities are significant, inaccuracies are expected. This is due to the mathematical structure of these models which uses a mapping strategy to form the internal (minor) hysteresis loops from the reference (major) curves. Since the mapping strategy only satisfies the initial and final point matching conditions for hysteresis segments, it does not necessarily force the inner loops to stay within the surrounding loops. Hence, when a system suffers from complex nonlinearities such as a butterfly-type response, significant modeling error may arise by the internal trajectories temporarily crossing the outer loops.

In order to generalize the present framework to a broader class of hysteretic systems, a more comprehensive model needs to be developed. This model must not only satisfy the initial and final point matching condition, but also generate the internal trajectories point by point to keep them bounded by their outer loops. To this end, we propose a recursive memory-based modeling approach that accurately describes various hysteretic systems. The logic of this strategy is based on an exponential convergence of the inner trajectories to their outer curves when targeting the previous turning points. The locations of the outer hysteresis loops are calculated recursively for every inner trajectory until arrival at the corresponding ascending or descending reference curve. Although the number of calculations increases compared to previously developed mapping-based strategies, the number of memory units remains the same. More importantly, the model is accurate for a broad range of systems, as long as the reference curves are accurately approximated with appropriate functions.

To demonstrate the effectiveness of the proposed strategy, we consider two solid-state smart actuators, a Galfenol-driven micropositioning actuator which exihibits butterfly-type hysteresis loops with large nonlinearities and a piezoelectric nanopositioning actuator which exhibits wide hysteresis loops and an underlying response which is nearly linear. In our investigation of these systems, hysteresis reference curves are approximated by polynomial functions, and the model parameters are identified to match experimental data. Results demonstrate accurate description of both minor and major hysteresis loops using the proposed recursive memory-based modeling framework for both the Galfenol and the piezoelectric actuator which have different hysteretic behaviors.

REVIEW OF MEMORY-BASED HYSTERESIS MODELING

A set of memory-based properties has been introduced in (Bashash and Jalili, 2006, 2007a, 2008) for accurate prediction of multiple-path hysteresis loops in piezoelectric materials. These properties, so-called 'targeting the turning points,' 'curve alignment,' and 'wiping out' effects at the turning points, pertain to trajectories with constant-rate quasi-static inputs, where the effects of system dynamics (e.g., inertia and damping) are negligible. In high-frequency operation, the hysteresis model can be integrated with actuator dynamics for effective positioning and control (Bashash and Jalili 2007b,c). In addition to the memory-based properties of hysteresis, which are used for the prediction of inner loops, reference curves play an important role in the modeling accuracy.

A hysteresis trajectory starts moving on the ascending reference curve, as schematically depicted in Figure 1. This curve can be approximated by a monotonically increasing continuous function. If the direction of the input changes when it reaches the maximum input threshold value, the trajectory breaks its path and moves downward on the descending reference curve, which can be approximated by another monotonically increasing continuous function. All the descending trajectories originating from the ascending reference curve converge to a single point called the lower convergence point (Figure 1).

Prediction of hysteresis response is performed by tracking a set of target points recorded from the past hysteresis trajectory. For the first ascending curve, the upper threshold point is the target point. If the input direction changes, the lower convergence point becomes the target for the first descending trajectory. For subsequent trajectories, the target points are the internal turning points at which the direction of input has changed. Consider for example a hysteresis trajectory which starts on the ascending reference curve as shown in Figure 2. The input direction changes at

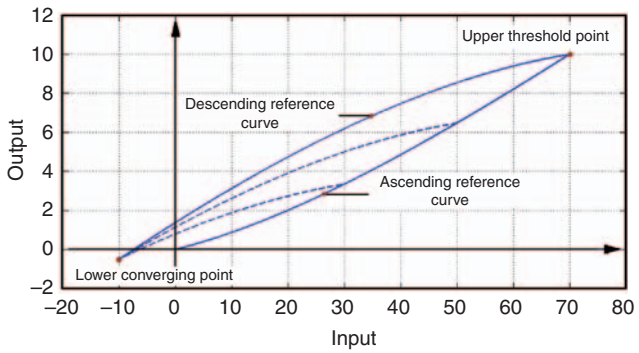

Figure 1. *Reference hysteresis curves.*

Point #2, and the trajectory targets the lower convergence point. The direction of input changes again at Point #3, and the trajectory targets the previous turning point, i.e., Point #2.

After reaching an internal turning point, the trajectory slightly bends and aligns to the previously broken curve associated with that turning point. This property, named *curve alignment*, enables precise tracking of the internal ascending or descending turning points, and is necessary for the prediction of multi-loop hysteresis response. A number of memory units are required to record the location of the target points and the internal turning points. In Figure 2, the trajectory that originats from Point #3 breaks its path after arriving at Point #2, and aligns to Curve 1-2 (the curve that connects Point #1 to Point #2); then it continues on Curve 1-2 towards its new target point, which is the upper threshold point. The dashed lines marked as 'non-aligned trajectory' demonstrate the divergence of hysteresis trajectory from its correct path, if the curve-alignment property is not applied at the turning point.

After reaching an internal turning point, the most recent closed loop associated with that turning point is no longer useful for the prediction of the subsequent hysteresis response. Therefore, the occupied memory units for that loop can be cleared. In other words, the memory units are wiped out when an internal hysteresis loop is closed. This property enables the use of a small number of memory units for predicting hysteresis loops with a large number of input variations and turning points.

Linear and nonlinear mapping strategies have been proposed in earlier formulations of the memory-based hysteresis modeling framework (Bashash and Jalili, 2006, 2008). Although these strategies are effective when the nonlinearities are small compared to the hysteresis looping effect (e.g., in piezoelectric actuators,) they lose accuracy when large nonlinearities are present as in magnetostrictive actuators. New strategies are required for precise modeling of hysteresis loops with large nonlinearities. In the next section, a novel recursive approach is proposed for generalizing the memory-based hysteresis modeling framework for a broad class of hysteretic systems.

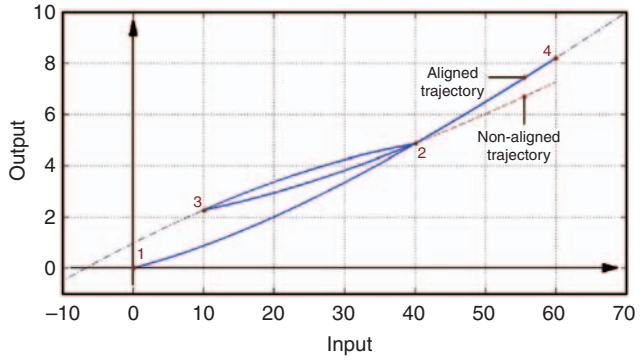

Figure 2. *Targeting turning point and curve alignment property.*

RECURSIVE MEMORY-BASED HYSTERESIS MODELING

In this section we propose a new approach for modeling hysteresis in smart materials and systems. We use a set of mathematical laws to adjust the convergence rate of internal hysteresis trajectories to their surrounding loops when they move toward target points. As shown in Figure 2, when a trajectory departs from a turning point, it gradually converges to its outer trajectory until they meet at the target point. We propose a *recursive memory-based approach*, to precisely model multiple loop hysteresis trajectories by controlling the convergence rate of internal hysteresis trajectories to their outer curves through a tunable exponential relation.

Figure 3 demonstrates a minor hysteresis loop (L_n, where L stands for "Loop" and the index n represents the loop number) inside of which another loop (L_{n+1}) is being formed. The objective is to derive a mathematical expression for L_{n+1} based on its surrounding loop, L_n, such that it converges to L_n as the input increases. For the $(n+1)$-th ascending curve $f^A_{n+1}(v)$, starting from the n-th lower turning point $\left(v^L_n, x^L_n\right)$ and targeting the n-th upper turning point $\left(v^U_n, x^U_n\right)$,

$$f^A_{n+1}(v) = f^A_n(v) + \Delta f^A_{n+1}(v), \tag{1}$$

where $\Delta f^A_{n+1}(v)$ is the distance of the $(n+1)$-th ascending trajectory from its previous ascending curve. Assuming exponential convergence, this distance can be expressed as

$$\Delta f^A_{n+1}(v) = \alpha_{n+1}\left(e^{k(v^U_n - v)} - 1\right), \tag{2}$$

where k is a tunable constant parameter shaping the hysteresis curve and α_{n+1} is a loop-varying parameter calculated by substituting the initial point $\left(v^L_n, x^L_n\right)$ into Equations (1) and (2):

$$\alpha_{n+1} = \frac{x^L_n - f^A_n\left(v^L_n\right)}{e^{k(v^U_n - v^L_n)} - 1}. \tag{3}$$

Figure 4 demonstrates the exponential convergence of $\Delta f^A_{n+1}(v)$ to zero as the input increases from the

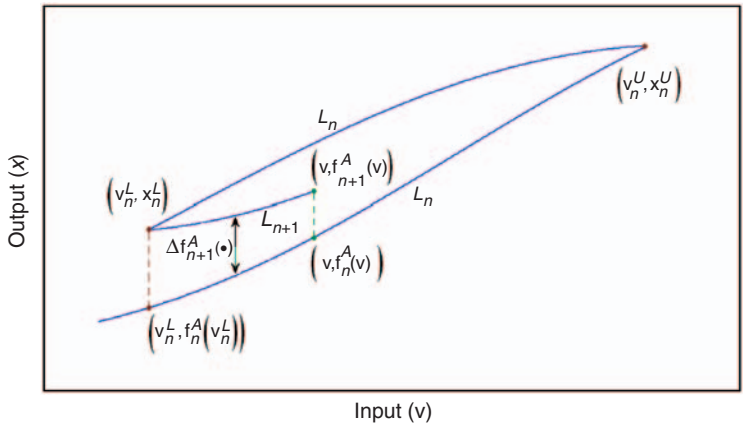

Figure 3. *A minor hysteresis loop being formed when the input increases from a lower turning point to an upper target point.*

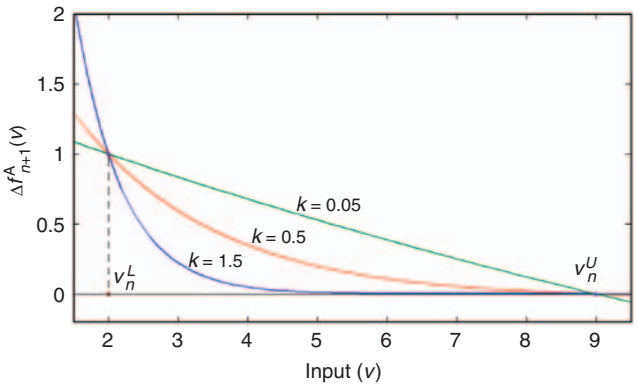

Figure 4. *Tunable exponential convergence of hysteresis loops.*

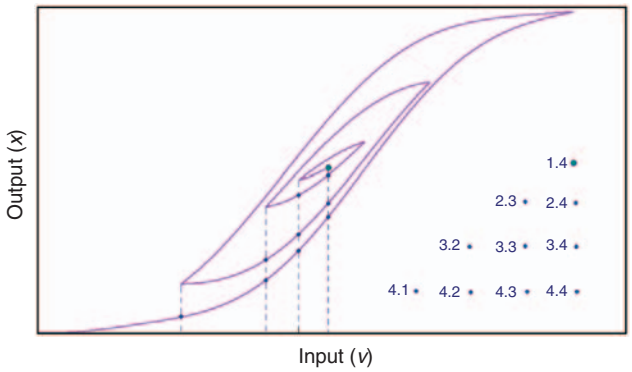

Figure 5. *Demonstration of all the points required to evaluate the model output at an instant of simulation, i.e., point 1.4 (figure shows the formation of the fourth inner loop, which requires a triangular matrix to be calculated).*

lower turning point v_n^L to the upper target point, v_n^U. Different values of k can result in different convergence rates.

Substituting Equation (3) into Equations (1) and (2), the following expression is obtained for the ascending hysteresis trajectory between the n-th upper and lower turning points:

$$f^A_{n+1}(v) = f^A_n(v) + \left(x^L_n - f^A_n\left(v^L_n\right)\right)\left\{\frac{e^{k(v^U_n - v)} - 1}{e^{k(v^U_n - v^L_n)} - 1}\right\}. \quad (4)$$

It is clear that both initial and target points are satisfied in Equation (4), i.e., $f^A_{n+1}(v^L_n) = x^L_n$ and $f^A_{n+1}\left(v^U_n\right) = f^A_n\left(v^U_n\right) = x^U_n$. This is a recursive expression for $f^A_{n+1}(v)$ due to the presence of $f^A_n(v)$ on the right side of the equation. Hence, to calculate each point of the hysteresis trajectory, all of the previous curves must be recursively calculated until reaching the corresponding reference curve. Since all the turning points are recorded in the memory unit, previous curves can be calculated from the turning points which have not been wiped out yet. Figure 5 depicts a multi-loop hysteresis trajectory and highlights the points needed for calculation of the present point. A lower triangular matrix with its dimension being equal to the number of inner loops must be formed in every simulation step. These points can be calculated from Equation (4) if all of the turning points in the history of the response have been recorded. As the number of minor loops increases, more computations must be performed to predict the hysteresis trajectories. Moreover, the precision of the model depends on the accuracy of the reference curves, which shape the entire hysteresis loops. Sufficiently high-order polynomials or exponential functions can ensure accurate approximation of reference curves in various hysteretic systems.

Once the hysteresis path from a turning to a target point is determined, it can be generalized for the prediction of a full hysteresis trajectory which may pass through all of the target points. A full ascending hysteresis path, starting from the n-th lower turning

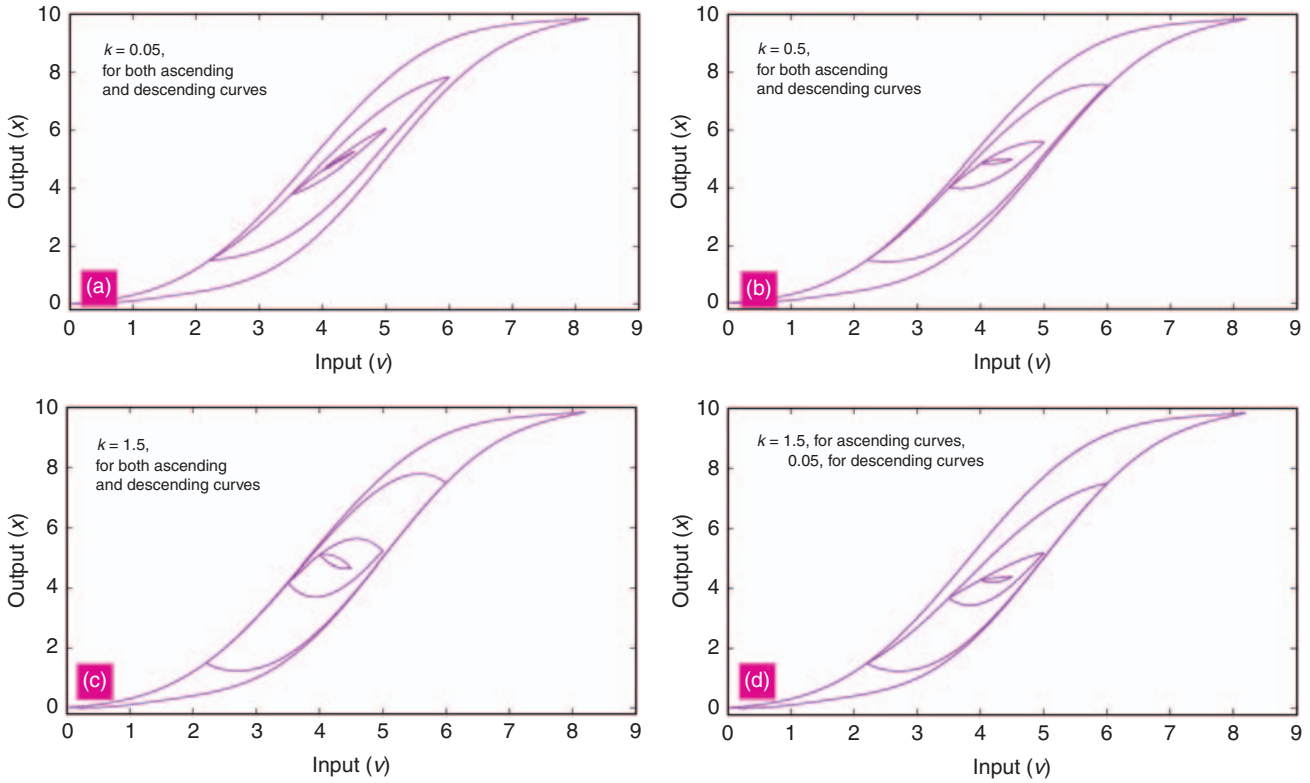

Figure 6. *Simulation of recursive memory-based hysteresis model for various values of parameter k: (a) k = 0.05, (b) k = 0.5, (c) k = 1.5, for both ascending and descending curves, and (d) k = 1.5 for ascending and k = 0.05 for descending curves.*

point and passing through all the target points until the upper threshold point is given by:

$$\begin{aligned} x^A_{n0}(v) &= f^A_{n+1}(v)H\left(v,v^L_n,v^U_n\right) + \sum_{i=1}^{n}\left[f^A_i(v)H\left(v,v^U_i,v^U_{i-1}\right)\right] \\ &= \left[f^A_n(v) + \left(x^L_n - f^A_n\left(v^L_n\right)\right)\left\{\frac{e^{k(v^U_n - v)}-1}{e^{k(v^U_n - v^L_n)}-1}\right\}\right] \\ &\quad \times H\left(v,v^L_n,v^U_n\right) + \sum_{i=1}^{n}\left[f^A_{i-1}(v) + \left(x^L_{i-1} - f^A_{i-1}\left(v^L_{i-1}\right)\right)\right. \\ &\quad \left.\times \left\{\frac{e^{k(v^U_{i-1} - v)}-1}{e^{k(v^U_{i-1} - v^L_{i-1})}-1}\right\}H\left(v,v^U_i,v^U_{i-1}\right)\right], \end{aligned} \tag{5}$$

where $x^A_{n0}(v)$ denotes the predicted multiple-segment hysteresis path, $f^A_0(v)$ represents the ascending reference curve, $\left(v^U_0, x^U_0\right)$ is the upper threshold point, and H represents the bilateral unit Heaviside function,

$$H(x,a,b) = \begin{cases} 1 & a \le x \le b \\ 0 & x > b \text{ or } x < a \end{cases}. \tag{6}$$

Similarly, one can obtain the full-path prediction of the $(n+1)$-th descending trajectory passing through all the target points until arriving at the lower threshold point,

$$\begin{aligned} x^D_{(n+1)0}(v) &= f^D_{n+1}(v)H\left(v,v^L_n,v^U_{n+1}\right) + \sum_{i=1}^{n}\left[f^A_i(v)H\left(v,v^L_{i-1},v^L_i\right)\right] \\ &= \left[f^D_n(v) + \left(x^U_{n+1} - f^D_n\left(v^U_{n+1}\right)\right)\left\{\frac{e^{k(v^L_n - v)}-1}{e^{k(v^L_n - v^U_{n+1})}-1}\right\}\right] \\ &\quad \times H\left(v,v^L_n,v^U_{n+1}\right) + \sum_{i=1}^{n}\left[f^D_{i-1}(v) + \left(x^U_i - f^D_{i-1}\left(v^U_i\right)\right)\right. \\ &\quad \left.\times \left\{\frac{e^{k(v^L_{i-1} - v)}-1}{e^{k(v^L_{i-1} - v^U_i)}-1}\right\}H\left(v,v^L_{i-1},v^L_i\right)\right]. \end{aligned} \tag{7}$$

Here we carry out a simulation to demonstrate the configuration of hysteresis loops obtained from the proposed framework. In the simulation, the reference curves are polynomials, and the multiple-peak input signal requires five memory units. Figure 6 demonstrates the response for different values of shaping parameter k. As k increases, inner loops converge faster to their surrounding loops resulting in wider hysteresis loops. Moreover, by different selection of k for the ascending and the descending curves, one can build an asymmetric hysteresis model (Figure 6(d)), which

may be desirable in practice. For a real system the parameter k cannot be larger than a limit that yields non-monotone curves similar to those presented in Figures 6(c) and (d).

EXPERIMENTAL ANALYSIS AND VALIDATION

In this section we investigate two hysteretic systems for experimental validation of the proposed framework: a Galfenol-driven micropositioning actuator and a piezoelectric nanopositioning stage. Galfenol exhibits large butterfly-type nonlinearity with little hysteresis, whereas in the piezoelectric stage hysteresis dominates the nonlinearity. Hence, the ability of the proposed framework to model a range of nonlinear and hysteretic systems is well examined.

Galfenol-driven Micropositioning Actuator

Magnetostriction (magnetically induced strain) and its complementary effect, stress-induced magnetization, originate from the coupling between inter-atomic spacing and magnetic moment orientation (DeSimone and James, 2002). Magnetostriction is thus a material property, which does not degrade with time or repetition of thermo-magneto-mechanical cycles. Magnetostrictive materials have facilitated dynamic actuators and sensors with robust operation, unlike ferroelectric materials, and broad frequency bandwidth, unlike shape memory materials.

Magnetostrictive Galfenol possesses key additional advantages; unlike most active materials, Galfenol is malleable and machinable (Kellogg et al., 2004) and can be safely operated under simultaneous tension, compression, bending, and shock loads. As a consequence of the unique combination of metallurgical and mechanical properties of Galfenol, this material can enable smart load-carrying Galfenol devices and structures with innovative 3D geometries manufactured by welding, extrusion, rolling, deposition, or machining. Furthermore, the unprecedented control of anisotropies through manufacturing and post-processing methods made possible with Galfenol (Wun-Fogle et al., 2005) can lead to innovative devices with fully coupled 3D functionality (Wun-Fogle et al., 2006). Despite these advantages, Galfenol does exhibit magnetic saturation, magnetic hysteresis and magnetomechanical nonlinearities, and accurate models describing the effect of magnetic field on strain are necessary for device design and control.

An experimental setup comprising a Galfenol-driven micropositioning actuator is shown in Figure 7. A unimorph beam consisting of a Galfenol laminate bonded to a brass laminate was placed in a magnetic circuit composed of steel flux paths driven by a copper coil. The Galfenol is research grade $Fe_{81.6}Ga_{18.4}$, which has been

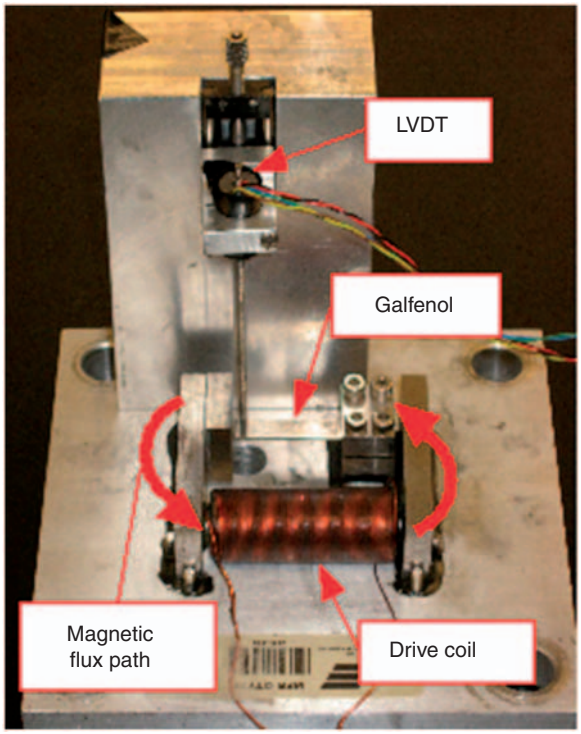

Figure 7. *Experimental setup for a Galfenol-driven micropositioning actuator.*

stress-annealed in order to pre-align magnetic domains perpendicular to the length of the beam thereby providing optimal magnetostriction (~200 ppm) along the beam length. When the coil is energized, a magnetic field causes the Galfenol to elongate while the brass laminate causes it to bend by restricting its elongation along the contact face. The coil is driven by an AE Techron LVC 5050 linear amplifier operated in voltage control mode. Current measurements are provided by the amplifier at a gain of 20 A/V and displacements are measured by a linear variable differential transformer (LVDT) instrument. The LVDT instrument comprises a Lucas Schaevitz MHR025 sensor and ATA-101 amplifier. A SignalCalc ACE dynamic signal analyzer from Data Physics Corporation simultaneously controls the drive coil amplifier and acquires the displacement and current measurements.

Major and nested minor loop tests were conducted using ramp inputs with a rate of 6 V/s and sampling frequency of 40 Hz. Closure of the minor loops suggests that dynamic effects are negligible for this rate of input. Figure 8 depicts the response of the actuator to the input current signal with a triangular profile. As seen in Figures 8(b) and (c), the response is nonlinear with a butterfly-shaped configuration and the looping effect due to magnetic hysteresis. From Figure 8(c), which shows the hysteresis loops between the applied current and the displacement, two important characteristics are observed, which will be considered in the model: (i) the

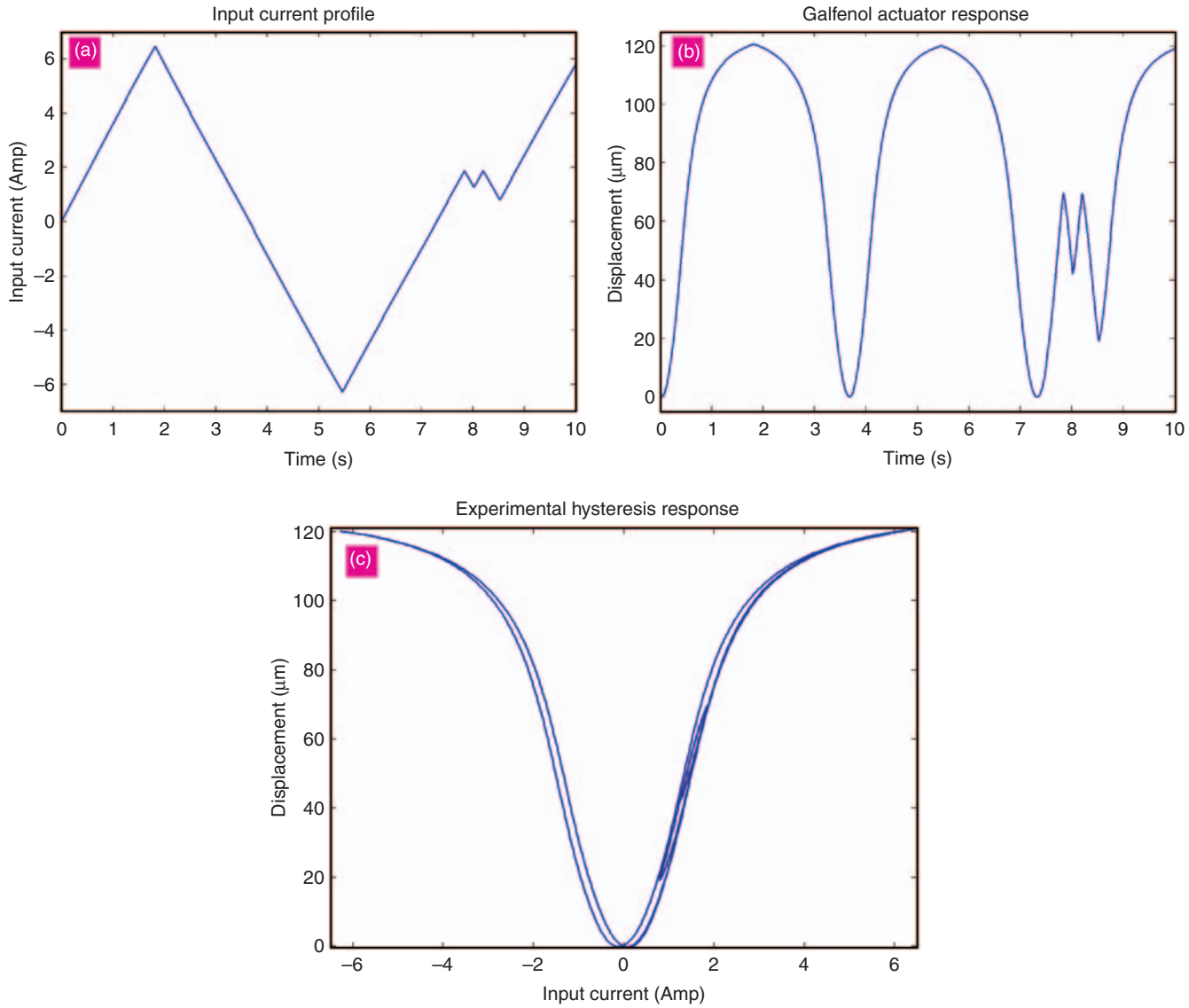

Figure 8. *Experimental response of Galfenol-driven micropositioning actuator: (a) input current profile, (b) resultant displacement, and (c) the butterfly hysteresis loops between the input current and the output displacement.*

hysteresis loops are symmetric with respect to the vertical axis, and (ii) the center of the loops is located at the origin. Therefore, the butterfly configuration can be reduced to a single-sided hysteresis configuration without the loss of generality and for the sake of simplicity.

Prior to applying the memory-based hysteresis model to this system, we assess the performance of a more convenient average model. In the average model, a tenth-order polynomial is averagely fitted to the ascending and descending reference curves (Figure 9(a)), resulting in an anhysteretic, non-linear model. Figure 9(b) depicts performance of the average model, where a large error is present because of neglecting the hysteresis effect.

In our application of the proposed memory-based hysteresis modeling framework, the ascending and descending curves are individually approximated through two tenth-order polynomials. Then, the convergence rates for the ascending and descending trajectories are separately identified through a single-parameter tuning procedure. Results are depicted in Figure 10. The model is able to precisely capture both major (Figure 10(a)) and minor (Figure 10(c) and (d)) hysteresis loops, with a small error trajectory (Figure 10(b)), having 0.84% maximum and 0.22% RMS values.

Piezoelectrically driven Nanopositioning Actuator

Piezoelectric actuators are well known for offering ultrafast and precise motions up to several hundreds of microns with sub-nanometer resolution. They are widely used in scanning probe microscopy for molecular and atomic scale imaging and manipulation (Curtis et al., 1997; Gonda et al., 1999), micro-robotics and microsurgery (Hesselbach et al., 1998; Akahori et al., 2005)

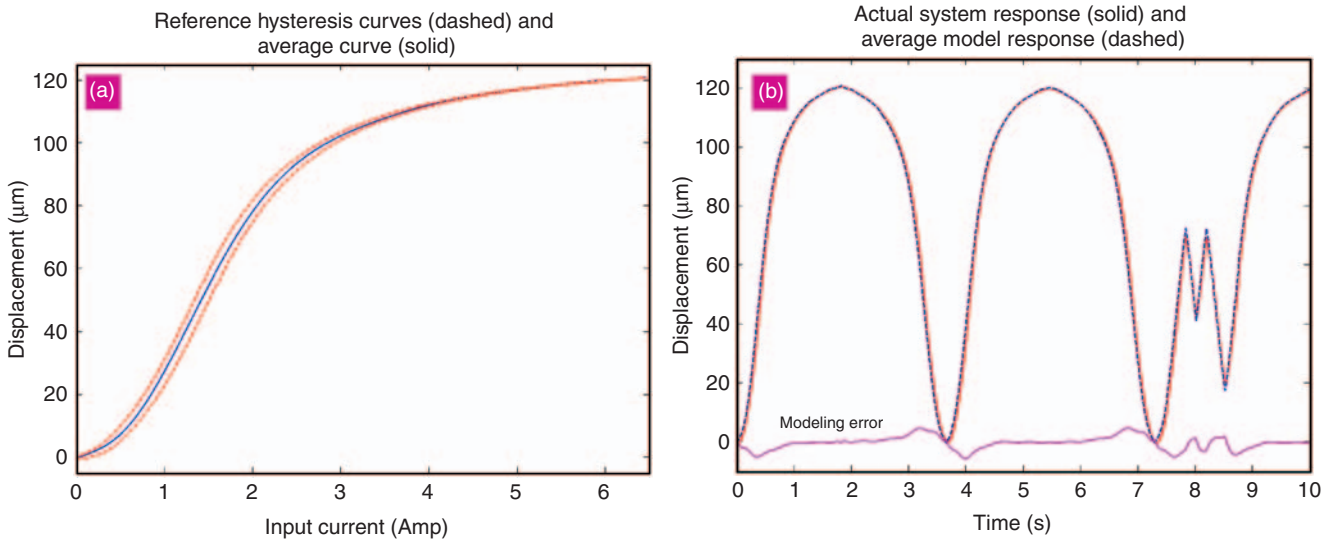

Figure 9. *Average model performance: (a) curve fitting to the experimental data, and (b) model response.*

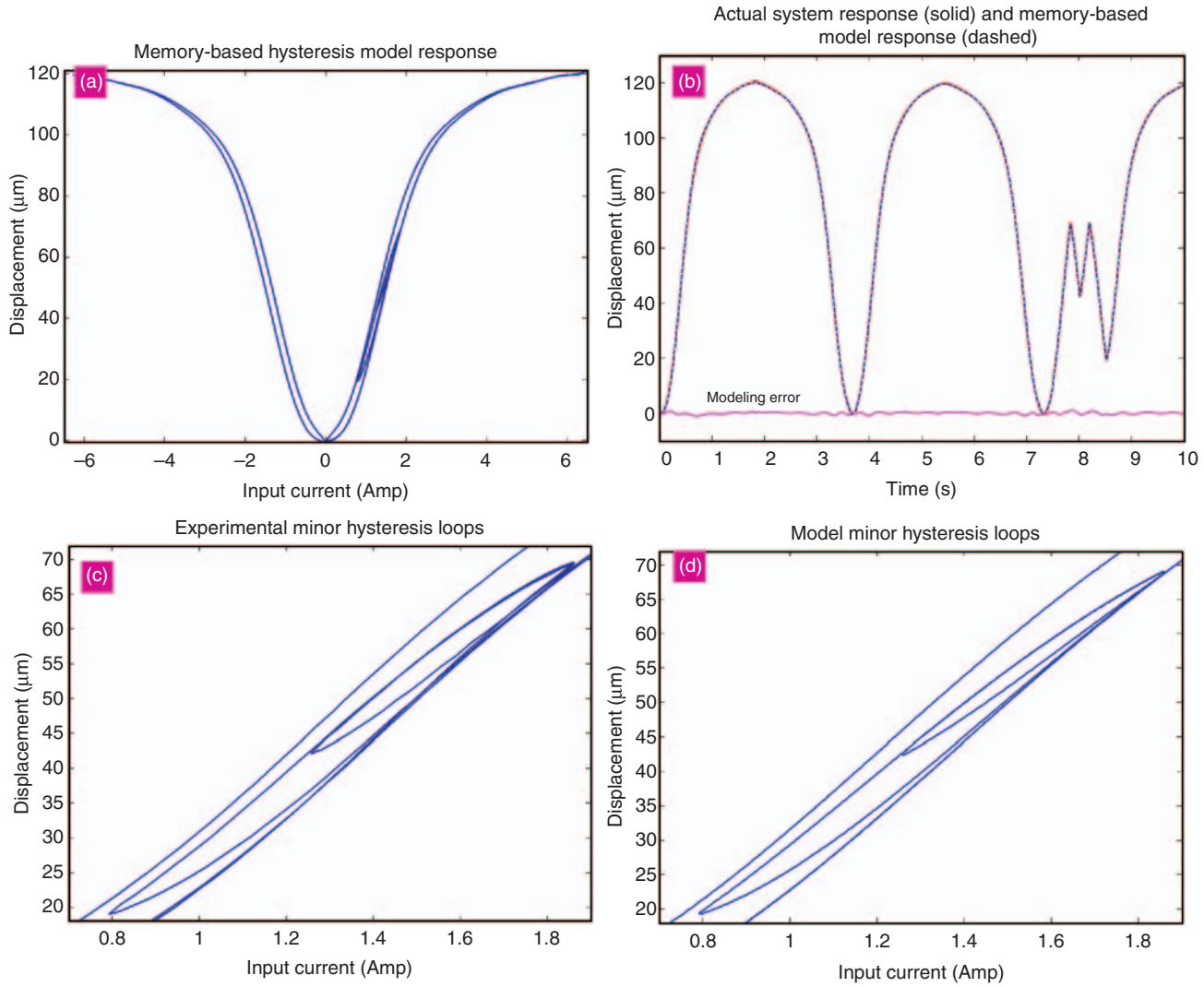

Figure 10. *Memory-based hysteresis model performance applied to the Galfenol micropositioner: (a) model response, (b) model comparison with the experiment, (c) experimental minor loops, and (d) model minor loops.*

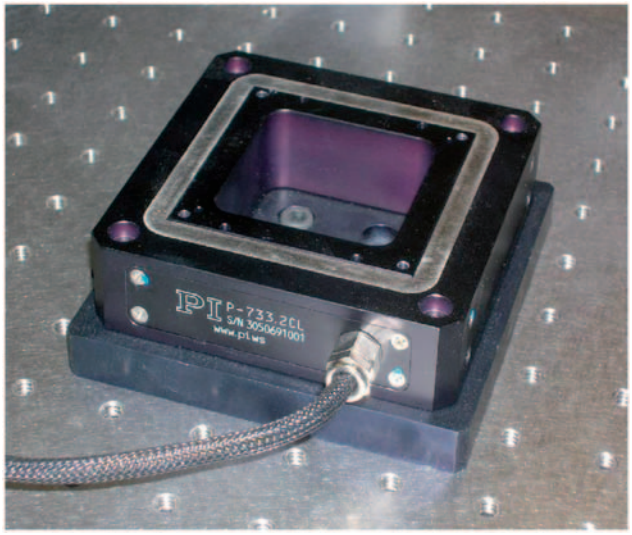

Figure 11. *Physik Instrumente P-733.2CL double-axis piezo-flexural nanopositioning actuator.*

photonics (Aoshima et al., 1992), and several other applications. However, similar to other smart materials, they exhibit a hysteretic response which highly degrades their performance.

Here we consider a Physik Instrumente P-733.2CL double-axis parallel piezo-flexure stage with high-resolution capacitive position sensors for another experimental validation of the proposed hysteresis modeling strategy (Figure 11). In our investigation, experimental data interfacing is accomplished with a Physik Instrumente E-500 chassis for the PZT amplifier and position servo-controller along with a DS1103 dSPACE® data acquisition and controller board, and the motions of the stage are measured by two built-in capacitive sensors with sub-nanometer resolution.

Figure 12 shows the experimental results. A triangular input voltage is applied to one of the stage axes (Figure 12(a)), and its response is captured by the corresponding position sensor (Figure 12(b)). The resultant hysteresis loops depicted in Figure 12(c) are wider

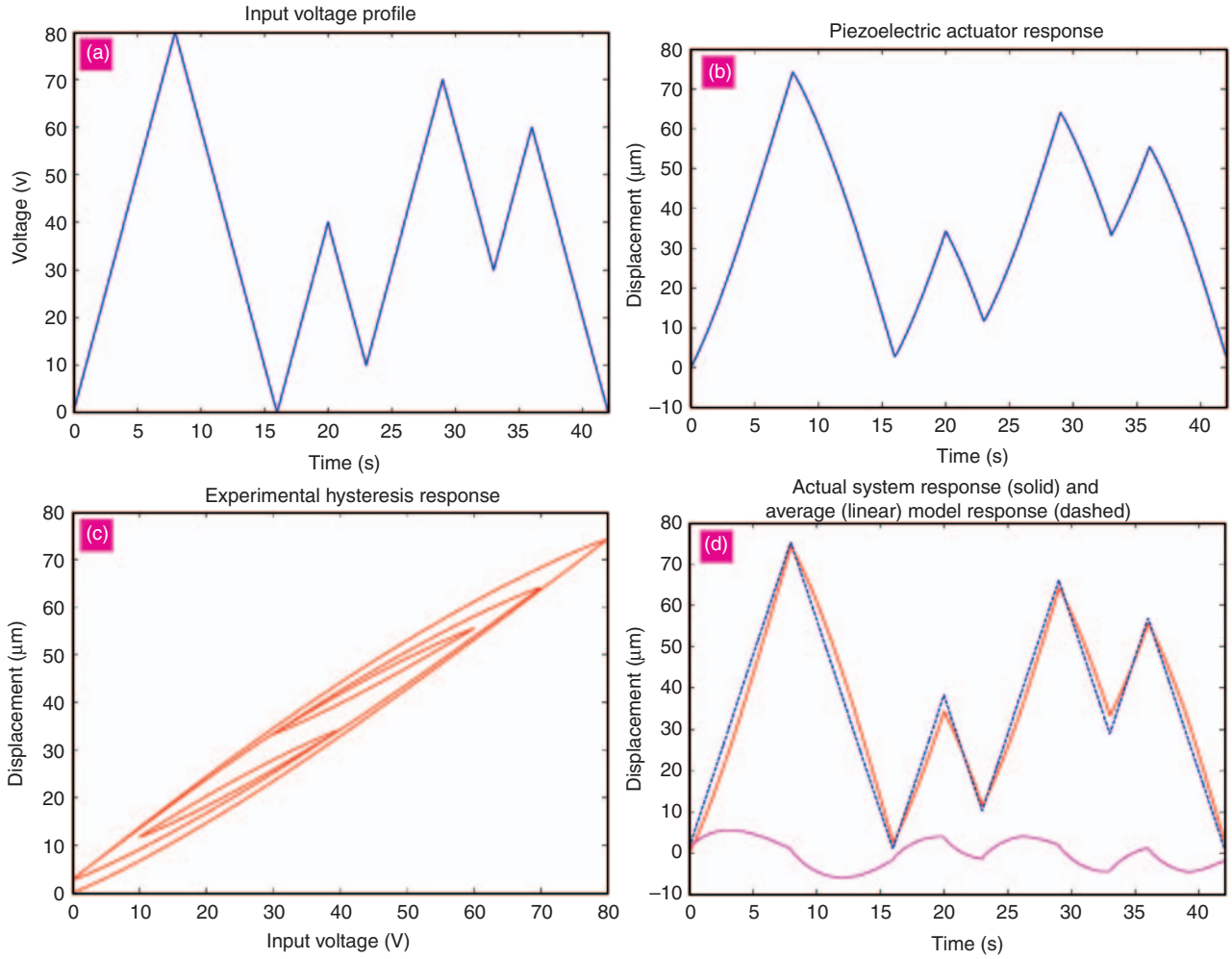

Figure 12. *Experimental response of the piezoelectric nanopositioning stage: (a) input voltage profile, (b) stage displacement, (c) resultant voltage–displacement hysteresis loops, and (d) performance of the average (linear) model.*

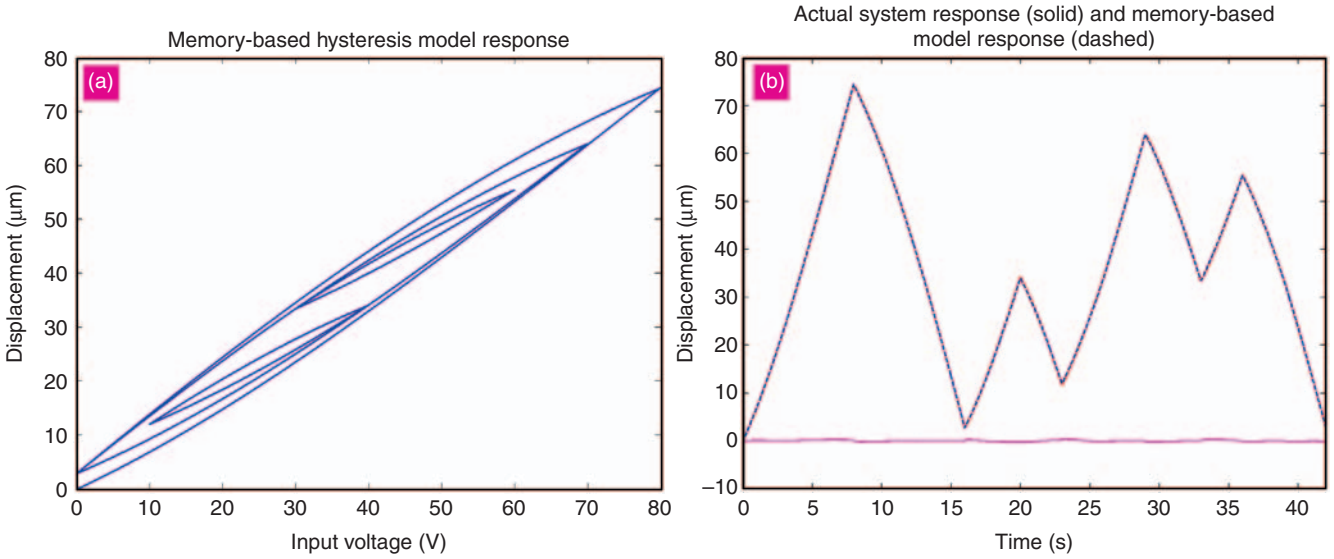

Figure 13. *Memory-based hysteresis model performance for the piezoelectrically driven system: (a) model response, and (b) comparison with the experiment.*

compared to those of the Galfenol actuator; however, their average can be approximated by a much lower order polynomial. Figure 12(d) demonstrates that a linear average model has a poor performance due to hysteresis. Hence, the need for a precise hysteresis model is clear for acquiring accurate positioning.

We adopt third-order polynomials to describe the ascending and the descending reference curve in application of the proposed recursive memory-based hysteresis model to the nanopositioning stage. The convergence rates for the ascending and the descending trajectories are separately identified through trial and error, and results are depicted in Figure 13. Achieving a small error trajectory with 0.45% maximum and 0.13% RMS values, the proposed hysteresis modeling approach demonstrates an effective implementation in piezoelectric-driven systems.

CONCLUSIONS

In this paper we proposed a recursive mathematical formulation for the memory-based hysteresis phenomenon observed in a broad class of smart structures and systems. For experimental validation, we investigated two different systems: a Galfenol-driven micropositioning actuator with small hysteresis but large butterfly-type nonlinearity, and a piezoelectric nanopositioning stage with small nonlinearity and large hysteresis. Our investigation demonstrated that significant improvements can be achieved in modeling accuracy by using this new hysteresis modeling strategy. The model precisely describes both major and minor hysteresis loops. Unlike previously developed memory-based hysteresis models, which are only applicable to piezoelectric actuators, the proposed strategy can be applied to a broader class of hysteretic systems with various nonlinearities.

ACKNOWLEDGMENT

PE and MJD wish to acknowledge Dr. Julie Slaughter of Etrema Products, Inc. for providing the Galfenol device utilized in this study and the financial support by the Office of Naval Research, MURI grant #N000140610530, Jan Lindberg program manager.

REFERENCES

Akahori, H., Haga, Y., Matsunaga, T., Totsu, K., Iseki, H., Esashi, M. and Wada, H. 2005. "Piezoelectric 2D Microscanner for Precise Laser Treatment in the Human Body," *3rd IEEE/EMBS Special Topic Conference on Microtechnology in Medicine and Biology*, May 2005, Oahu, Hawaii, pp. 166–169.

Aoshima, S., Yoshizawa, N. and Yabuta, T. 1992. "Compact Mass Axis Alignment Device with Piezo Elements for Optical Fibers," *IEEE Photonics Technology Letters*, 4:462–464.

Bashash, S. and Jalili, N. 2006. "Underlying Memory-dominant Nature of Hysteresis in Piezoelectric Materials," *Journal of Applied Physics*, 100:014103.

Bashash, S. and Jalili, N. 2007a. "Intelligent Rules of Hysteresis in Feedforward Trajectory Control of Piezoelectrically-driven Nanostages," *Journal of Micromechanics and Microengineering*, 17:342–349.

Bashash, S. and Jalili, N. 2007b. "Modeling of Piezo-flexural Nanopositioning Systems Subjected to Rate-varying Inputs," *Proceedings of 14th SPIE Annual Symposium on Smart Structures and Materials*, San Diego, CA, March 2007.

Bashash, S. and Jalili, N. 2007c. "Robust Multiple-frequency Trajectory Tracking Control of Piezoelectrically-driven Micro/Nano Positioning Systems," *IEEE Transactions on Control Systems Technology*, 15:867–878.

Bashash, S. and Jalili, N. 2008. "A Polynomial-based Linear Mapping Strategy for Compensation of Hysteresis in Piezoelectric

Actuators," *ASME Transactions, Journal of Dynamic Systems, Measurements and Control*, 130:0310081–10.

Curtis, R., Mitsui, T. and Ganz, E. 1997. "Ultrahigh Vacuum High Speed Scanning Tunneling Microscope," *Review of Scientific Instruments*, 68:2790–2796.

DeSimone, A. and James, R.D. 2002. "A Constrained Theory of Magnetoelasticity," *Journal of Mechanics and Physics of Solids*, 50:283–320.

Goldfarb, M. and Celanovic, N. 1997. "A Lumped Parameter Electromechanical Model for Describing the Nonlinear Behavior of Piezoelectric Actuators," *Transactions of the ASME, Journal of Dynamic Systems, Measurement, and Control*, 119:478–485.

Gonda, S., Doi, T., Kurosawa, T., Tanimura, Y., Hisata, N., Yamagishi, T., Fujimoto, H. and Yukawa, H. 1999. "Accurate Topographic Images Using a Measuring Atomic Force Microscope," *Applied Surface Science*, 144–145:505–509.

Hesselbach, J., Ritter, R., Thoben, R., Reich, C. and Pokar, G. 1998. "Visual Control and Calibration of Parallel Robots for Micro Assembly," *Proceedings of SPIE*, Vol. 3519, Boston, MA, Novermber 1998, pp. 50–61.

Kellogg, R.A., Russell, A.M., Lograsso, T.A., Flatau, A.B., Clark, A.E. and Wun-Fogle, M. 2004. "Tensile Properties of Magnetostrictive Iron-Gallium Alloys," *Acta Materialia*, 52:5043–5050.

Krasnosel'skii, M.A. and Pokrovskii, A.V. 1989. *Systems with Hysteresis*, Springer-Verlag, New York.

Kuhnen, K. and Janocha, H. 2001. "Inverse Feedforward Controller for Complex Hysteretic Nonlinearities in Smart-material Systems," *Control and Intelligent Systems*, 29:74–83.

Ping, G. and Musa, J. 1997. "Generalized Preisach Model for Hysteresis Nonlinearity of Piezoceramic Actuators," *Precision Engineering*, 20:99–111.

Smith, R.C. 2005. *Smart Material Systems: Model Development*, Frontiers in Applied Mathematics Series, SIAM.

Smith, R.C., Dapino, M.J. and Seelecke, S. 2003a. "A Free Energy Model for Hysteresis in Magnetostrictive Transducers," *Journal of Applied Physics*, 93:458–466.

Smith, R.C., Seelecke, S., Ounaies, Z. and Smith, J. 2003b. "A Free Energy Model for Hysteresis in Ferroelectric Materials," *Journal of Intelligent Material Systems and Structures*, 14:719–739.

Smith, R.C., Seelecke, S., Dapino, M.J. and Ounaies, Z. 2006. "A Unified Model for Hysteresis in Ferroic Materials," *Journal of Mechanics and Physics of Solids*, 54:46–85.

Stepanenko, Y. and Su, C.Y. 1998. "Intelligent Control of Piezoelectric Actuators," *Proceedings of 37th IEEE Conferenceon Decision and Control*, 4:4234–4239.

Tan, X. and Baras, J.S. 2004. "Modeling and Control of Hysteresis in Magnetostrictive Actuators," *Automatica*, 40:1469–1480.

Wun-Fogle, M., Restorff, J.B., Clark, A.E., Dreyer, E. and Summers, E. 2005. "Stress Annealing of Fe–Ga Transduction Alloys for Operation Under Tension and Compression," *Journal of Applied Physics*, 97:10M301.

Wun-Fogle, M., Restorff, J.B. and Clark, A.E. 2006. "Magnetomechanical Coupling in Stress-annealed Fe-Ga (Galfenol) Alloys," *IEEE Transactions on Magnetics,* 42(10): pp. 3120–3122.